DOAS-4R ultraviolet open path gas analyzer

S.S. Khmelevtsov, V.A. Korshunov, and A.M. Vdovenkov

Scientific Production Association "Taifun," Obninsk, Kaluga Region

Received April 26, 2002

An ultraviolet open path gas analyzer operating in the 200–460 nm wavelength range designed for determining low concentrations of gaseous pollutants in the urban atmosphere based on differential optical absorption spectroscopy (DOAS). The analyzer includes a xenon arc lamp, coaxial telescope, retroreflector, monochromator-spectrograph, and linear diode array as a detector. A personal computer is used for measurement control and data processing. The analyzer's databank contains 31 gaseous components, including such ubiquitous pollutants as sulfur dioxide, nitric oxide, nitrogen dioxide, ozone, formaldehyde, ammonia, and some monocyclic hydrocarbons. Minimum detectable concentrations vary from fractions of ppb to a few ppb. Results of trial measurements in Obninsk are presented.

Introduction

The *differential optical absorption spectroscopy* (DOAS) method is now widely used for measuring minor concentrations of atmospheric pollutants. First measurements based on the DOAS principles were conducted in the late 1970s. After that, this method has been extensively employed in both research and applied studies connected with monitoring of atmospheric pollution. The DOAS principles are reviewed and analyzed in Ref. 1. In a wide sense, differential methods in spectroscopy mean any measurement based on comparison of spectral characteristics for two or several wavelengths. In this paper, the DOAS method is understood in a more narrow sense[1] as a method based on a representation of an absorption spectrum as a sum of smooth and differential components and on the analysis of the differential absorption spectrum as a whole for the selected wavelength region. At a precision recording of a spectrum by DOAS method, it is important to exclude any signal variations that are not associated with the absorption spectra of the gases analyzed. Therefore, either fast scanning of the spectrum with moving slits or simultaneous recording of all spectral components in the selected region with a multichannel detector is used.

Purely optical DOAS measurements have many advantages as compared with ordinary contact methods. In particular, they require no sampling and use no chemical materials. Besides, they are capable of measuring simultaneously and automatically several gaseous components, and the time for one measurement usually is only 2–3 min.

Some commercial DOAS analyzers for monitoring of atmospheric pollution have been recently developed in foreign countries. In Russia, DOAS analyzers have been developed since 1997 by the Scientific Technical Center "Eridan-1" (Obninsk). In this paper, we describe the latest DOAS-4R model of the gas analyzer, which was certified by the Russian State Standardization Committee in 2001, discuss the measurement technique, and present the results of field measurements of some gaseous atmospheric constituents in Obninsk.

Operating principle

The DOAS-4R gas analyzer is designed for determining low concentrations of gaseous pollutants in the atmosphere. It operates in the wavelength region from 200 to 460 nm. Depending on the gas concentrations and the spectral interval taken in the selected region, the path length can vary from several meters to 1 km. The appearance of the DOAS-4R gas analyzer is shown in Fig. 1. The DOAS-4R operating principle is illustrated in Fig. 2.

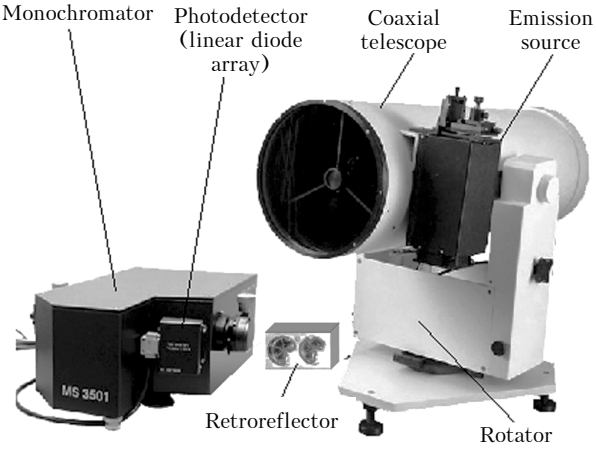

Fig. 1. External view of the DOAS-4R open path gas analyzer.

For operation in the atmosphere, a telescope with integrated transmitting and receiving channels is used. The telescope is fixed on a biaxial rotator. The luminous body of a 150 W xenon arc lamp is placed near the focus of the main spherical mirror. The ring-shaped radiation beam is directed by a plane beam turning mirror and the periphery of spherical mirror along the atmospheric path to a retroreflector. The inner ring of the spherical mirror is used for reception of the radiation reflected by the retroreflector. With the secondary turning mirror, the received radiation is directed through the central hole in the spherical mirror to the entrance aperture of a fiber-optics cable that is also located near the focus of the spherical mirror. The fiber-optics cable transports the

0235-6880/02/11 907-06 $02.00

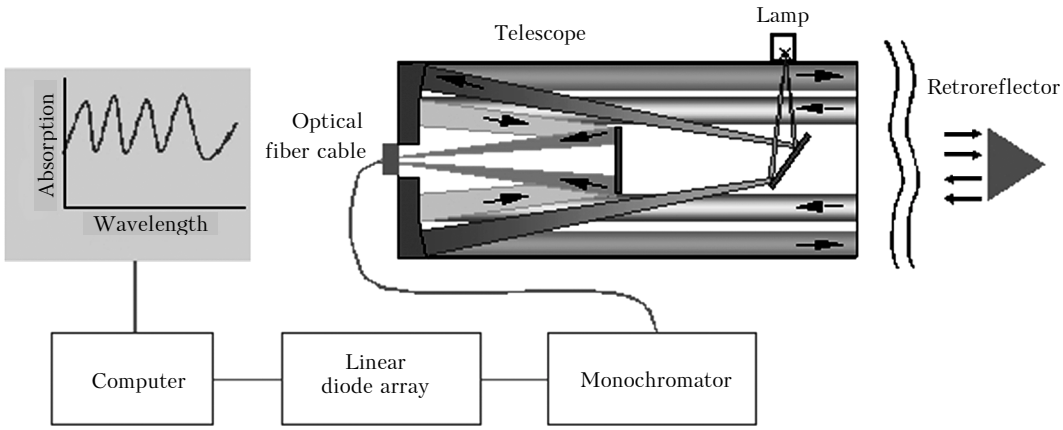

Fig. 2. Operating principle of the DOAS-4R open path gas analyzer.

radiation to the entrance slit of a monochromator-spectrograph (MS). A linear photodiode array is installed in the plane field of the MS exit image. The signal from the array is digitized and entered into a computer for processing. Note that the photodiode array operates at room temperature without cooling.

To record the xenon lamp spectrum, the entrance aperture of the telescope is shut with a cover to prevent exit of the radiation. A retroreflector similar to that installed at the far end of the path is placed inside the cover at the boundary between the telescope's receiving and transmitting zones. The retroreflector reflects a part of the lamp radiation into the receiving ring of the telescope's spherical mirror.

Below we present the basic performance parameters of the DOAS-4R units. The main spherical mirror of the telescope has the diameter of 261 mm and the focal length of 800 mm. The retroreflector 60 mm in diameter is made of quartz with the mutual orientation of the reflecting planes accurate to 5″. Quartz monofiber with the diameter of 200 μm in a protecting cover is used as a light guide. An important parameter is homogeneity of the angular distribution of radiation at the exit from the light guide, since inhomogeneities in the angular distribution can lead to appearance of parasitic structures in the spectral signal.[2] Tests showed that a smooth bell-shaped radiation distribution with the halfwidth of 15° is observed at the exit of the light guide used in the DOAS-4R.

The high-accuracy MS-3501 I monochromator-spectrograph (SOLAR TII, Minsk, Belarus) has 3.8 F/D ratio and the inverse linear dispersion of 2.4 nm/mm. The MS uses a diffraction grating with the maximum reflection at the wavelength of 275 nm. A Hamamatsu 1024-pixel 25 × 500 μm linear diode array is set in the 28 × 10 mm plane MS field. The diode array simultaneously records the spectrum in the wavelength interval of 60 nm with the resolution of 0.24 nm at the slit width of 100 μm. The time of the exposure needed for single recording of the spectrum can vary from 10 ms to 5 s. Usually, the results are averaged over 100–1000 exposures with the total time no longer than 3 min. The electronic unit of the diode array includes an analog-to-digital converter (ADC). The electronic unit card is set in a free ISA slot of the computer. The DOAS-4R is operated in a computer-controlled and fully automated measurement mode with the possibility of sharing the results via a communication line.

Measurement method

When processing measurements, the spectrum of the signal having passed through the atmosphere is normalized to the spectrum of the source and then separated into the fast varying (differential) and smoothly varying parts.[1] This separation is conditional to some extent and depends on the representation of the smoothly varying component. In this paper, we represent the smoothly varying part as a polynomial, therefore that part of the considered characteristic (signal, cross section), which can be represented as a polynomial in the considered wavelength interval, is classified as a polynomial part, and the rest is classified as a differential part.

Smooth variation of the signal accounts for Rayleigh and aerosol scattering, as well as continuum absorption by gases present in the atmosphere. It also includes instrumental components, for example, transmittance of the optical elements and the spectral characteristic of the detector. The differential part in the considered spectral region is caused by the absorption due vibronic molecular transitions. Overlapping of some vibrational bands in the absorption spectrum creates a spectral absorption curve characteristic of every gas, and this allows identification of components in a gas mixture and determination of their concentrations.

In the DOAS method, it is assumed that either the source and instrumental spectral dependences include no differential component or it is completely excluded by normalization. For some reasons whose analysis is beyond the scope of this paper, a small ($10^{-2} - 10^{-3}$) differential component of this kind is still present and not fully excluded at signal normalization to the lamp spectrum. The residual differential component, along with the instrumental noise, determines the measurement error including both the random and unknown systematic components.

The normalized signal of the DOAS analyzer $S(\lambda)$ can be written as

$$S(\lambda) = A(\lambda) \int_{-\infty}^{+\infty} G(|\lambda' - \lambda|)\ T_{O_2}(\lambda') \times$$

$$\times \exp\left[-\sum_i \sigma_{gi}(\lambda')\, C_i L \right] B(\lambda')\, d\lambda', \qquad (1)$$

where $G(|\lambda' - \lambda|)$ is the instrumental function; $A(\lambda)$ is the spectral sensitivity of the detector; C_i is the concentration of the ith component of a gas mixture; $\sigma_{gi}(\lambda')$ is the absorption cross section of the ith component; L is the path length, which is understood here as a dual path length (for the two-pass scheme, the doubled distance from the telescope to the retroreflector); $B(\lambda')$ is the smoothly varying part of the optical signal at the entrance of the spectrometer; $T_{O_2}(\lambda') = \exp[\sigma_{O_2}(\lambda')\, C_{O_2} L]$ is the spectral transmission coefficient of oxygen at the path having the length L with the concentration of oxygen molecules C_{O_2}.

It should be noted that both the total and the differential absorption cross sections could be used as $\sigma_{gi}(\lambda')$. In the latter case, absorption due to the smoothly varying part of the cross section is taken into account when approximating the signal by a polynomial.

Consider first the wavelength region, in which absorption by oxygen can be neglected. Then, with the additional assumptions on the small optical absorption thickness for every gas $\sigma_{gi}(\lambda')\, C_i\, L \ll 1$ and smooth variation of $B(\lambda')$ on the scale of the instrumental function $G(|\lambda - \lambda'|)$, we can pass from Eq. (1) to a linear equation convenient for mathematical processing. Write it in a discrete form with the allowance made for the polynomial representation of the smooth part

$$S_k = \sum_{j=0}^{N} A_j \lambda_k^j - L \sum_{i=1}^{m} C_i F_{k,i} \qquad k = 1, \ldots, n, \qquad (2)$$

where $S_k = \ln S(\lambda_k)$; $F_{k,i} = \sigma_i(\lambda_k)$, $\sigma_i(\lambda_k)$ is the result of convolution of the initial cross section $\sigma_{gi}(\lambda_k)$ with the instrumental function; n is the number of discrete signal readings; m is the number of gaseous components; N is the polynomial power; A_j are the polynomial coefficients.

Let us present Eq. (2) in the matrix form

$$S_k = \sum_{i=1}^{p} D_{ki} X_i\,, \quad k = 1, \ldots, n, \qquad (3)$$

where D_{ki} is the matrix for the system of equations (2); the vector X_i is $X_i = (A_0, A_1, \ldots, A_N, C_1, \ldots, C_m)$; $p = N + m + 1$.

The system of equations (3) is solved using a numerical method of singular matrix decomposition,[3] which provides for better numerical stability as compared with the frequently used method of normal equations. The matrix $\mathbf{D}$ in this case is represented as $\mathbf{D} = \mathbf{U\Sigma V}^{\mathrm{T}}$, where $\mathbf{U}$ and $\mathbf{V}$ are orthogonal matrices, and $\mathbf{\Sigma}$ is the diagonal matrix with singular numbers ν_i at the main diagonal. Within this representation, the solution by the least squares method for the components of the vector X_i can be written as follows:

$$X_i = \sum_{k=1}^{p} V_{ik}\, z_k; \quad z_k = \frac{d_k}{\nu_k}; \quad d_k = \sum_{i=1}^{n} U_{ik} S_i. \qquad (4)$$

Assume that the covariance error matrix $\langle \delta S_i\, \delta S_k \rangle$ is diagonal and all diagonal elements are ε^2 (where ε is the relative measurement error).

Then from Eq. (4) we obtain estimates for variances of the parameters X_i:

$$\langle \delta X_i^2 \rangle = \varepsilon^2 \sum_{k=1}^{p} \frac{V_{ik}^2}{\nu_k^2}, \quad i = 1, \ldots, p. \qquad (5)$$

In the measurement process, ε can be estimated from deviations, i.e., root-mean-square differences between the measured and calculated signals S_k.

Allowance for the oxygen absorption

The wavelength region from 240 to 300 nm includes structured absorption bands for some monocyclic hydrocarbons polluting the atmosphere. It also includes the range of oxygen absorption from 240 to 280 nm. In this range, the differential optical absorption thickness of oxygen for atmospheric paths of several hundreds meters long can reach ~ 0.1–0.2, while the minimum detectable absorption thickness for DOAS measurements is ~ 10^{-4} – 10^{-3}. Therefore, oxygen absorption in the spectral range of 240–280 nm should be carefully taken into account. As to the continuum absorption in the wavelength region $\lambda \le 242$ nm, oxygen absorption here is taken into account by the approximating polynomial because of the smooth wavelength dependence of the absorption cross section, and thus it does not affect measurement results.

The absorption spectrum of atmospheric oxygen in the region of 240–280 nm includes the Herzberg bands I, II, and III, which consist of discrete absorption bands observed against the background of the Wulf diffuse absorption band.[4]

Diffuse absorption in the Wulf band is connected with the Herzberg band III and, as was shown in Ref. 4, caused by pair collisions of oxygen molecules with other molecules in the air (largely, oxygen and nitrogen molecules). The distinguishing feature of absorption in the Wulf band is the square pressure dependence of the optical absorption thickness that corresponds to the collisional nature of absorption.[4]

Most careful measurements of oxygen absorption performed in recent years are published in Refs. 5 and 6. Reference 5 presents the positions of rotational lines for all the three Herzberg bands, and Ref. 6 presents the line strengths for the same rotational transitions. Line broadening at atmospheric pressure is caused by both the Doppler effect and collisional processes. As known,

the line profile $g(\nu - \nu_0)$ in this case is described by the Voigt integral.

The total oxygen absorption cross section can be presented as a sum of contributions from discrete lines with the intensity S_i at the frequency ν_{0i} and the continuum absorption in the Wulf band $\sigma_W(\nu)$:

$$\sigma_{O_2}(\nu) = \sum_i S_i \, g(\nu - \nu_{0i}) + \sigma_W(\nu), \qquad (6)$$

where summation is performed over all lines contributing markedly to absorption at the frequency ν.

It can be shown that in the presence of absorption by oxygen Eq. (1) can also be reduced to the form (2), if oxygen is included in the list of gases to be determined with the effective absorption cross section $\sigma_{O_2}^{eff}$, where

$$\sigma_{O_2}^{eff}(\nu) = -\frac{1}{C_{O_2} L} \ln\left[\int_{-\infty}^{+\infty} G(|\nu' - \nu|) T_{O_2}(\nu') \, d\nu'\right]. \qquad (7)$$

It should be noted that the effective cross section $\sigma_{O_2}^{eff}$ is calculated for the given values of the path length, atmospheric temperature and pressure.

We have compared the measurement results in the minimum polluted atmosphere with calculations in the region of 240–270 nm. In the comparison, we took into account only oxygen and ozone, while the concentrations of other gaseous components contributing to absorption in this region, e.g. benzol and toluene, were assumed negligibly small. As a result, the discrepancy was $4 \cdot 10^{-3}$. At the optical absorption thickness ~ 0.1 on the path, the obtained discrepancy was close to the experimental error in line intensities ~ 2% given in Ref. 6. Analysis of the discrepancies obtained in a rather long series of measurements conducted on different days showed that these discrepancies have a significant systematic component δR and the random component, whose root-mean-square value was 10^{-3}. The parameter $\delta\sigma_{O_2} = \delta R/(C_{O_2} L)$ was interpreted as an empirical correction to the oxygen absorption cross section and introduced in calculations in the further experiments. The resulting measurement error $\approx 10^{-3}$ is quite acceptable for determination of the concentrations of monocyclic hydrocarbons under urban conditions.

Minimum detectable concentrations and examples of field measurements

The list of gases included now in the analyzer's databank consists of 31 species, among them such ubiquitous atmospheric pollutants as NO_2, NO, SO_2, O_3, CH_2O, NH_3, as well as NOHO, CS_2, CH_3COH, benzol, toluene, phenol, and other compounds from the class of monocyclic hydrocarbons, whose absorption cross sections were published in Ref. 7. For concentration determination, all the above gases (except for NOHO) are distributed over five 60-nm wide spectral intervals. Up to 15 gases can be determined simultaneously.

As a minimum detectable concentration (MDC), we took 3σ, where $\sigma = \langle \delta X^2 \rangle^{1/2}$ was calculated by Eq. (5). The error in signal recording ε entering into Eq. (5) was estimated from the discrepancies obtained at measurements in the atmosphere. The values of ε were $2 \cdot 10^{-4}$ and 10^{-3} as the spectral interval for measurements was selected in the wavelength range longer or shorter than 280-nm wavelength. The increase of the discrepancy in the range of 240–280 nm is caused, first, by the influence of errors in absorption by atmospheric oxygen. In the range of 210–240 nm, the discrepancies increased because of the decrease in the signal due to the decreasing output of the xenon lamp in this spectral range and increasing atmospheric absorption.

The Table presents the calculated values of MDC for some ubiquitous atmospheric pollutants along with the wavelength ranges optimal for measurements and daily mean maximum permissible concentrations (MPC_{dm}) established in Russia for these gases. The calculation was performed for the path length of 400–500 m for all gases except for CH_2O (for which the path length was 1000 m). It was assumed that the spectrum was recorded in a 60-nm interval with the resolution of 0.3 nm and the signal acquisition time of 2–3 min. For other gases, we have obtained MDC ranging from 0.1 to 2.7 ppb.

Minimum detectable concentrations for some ubiquitous gases

Gas		Wavelength, nm	MDC, ppb	MPC_{dm}, ppb
NH_3	Ammonia	210–230	0.8	50
NO	Nitric oxide	210–230	1.8	45
NO_2	Nitrogen dioxide	320–460	1.0	20
SO_2	Sulfur dioxide	280–320	0.2	20
O_3	Ozone	250–270	3.0	14
CH_2O	Formaldehyde	280–350	1.0	2
C_6H_6	Benzol	236–263	0.9	30
C_7H_8	Toluene	250–270	1.5	150

In the period from April 24 to May 11 of 2001, field tests of the DOAS-4R, including measurements in Obninsk, were conducted. Figure 3 depicts the measured absorption spectra for several spectral intervals compared with the calculated data. Figure 4 exemplifies simultaneous measurements of the concentrations of SO_2, CH_2O, NO_2, and O_3 in the region of 295–350 nm. The measurements were conducted during 24 hours on May 7 and 8. The zero nighttime concentrations mean that the actual concentrations of the gases at that time were lower than MDC.

Analysis of these and other measurements showed that the maximum concentrations were observed at the time, when the wind was directed from potential sources of the measured gases. As to the diurnal behavior of the concentration of some gases, we can note the following:

– SO_2. A morning peak of 1–2 ppb (7 ppb on one day) was observed. The rest diurnal behavior was rather arbitrary.

– CH_2O. No typical diurnal behavior was observed. Concentration peaks up to 5 – 8 ppb were observed at

any time. This is likely connected with both alternation of wind direction and changes in emissions of this pollutant with time.

– NO_2. The obtained diurnal behavior is rather typical[8]; it includes morning and evening peaks, as well as midday and nighttime minima.

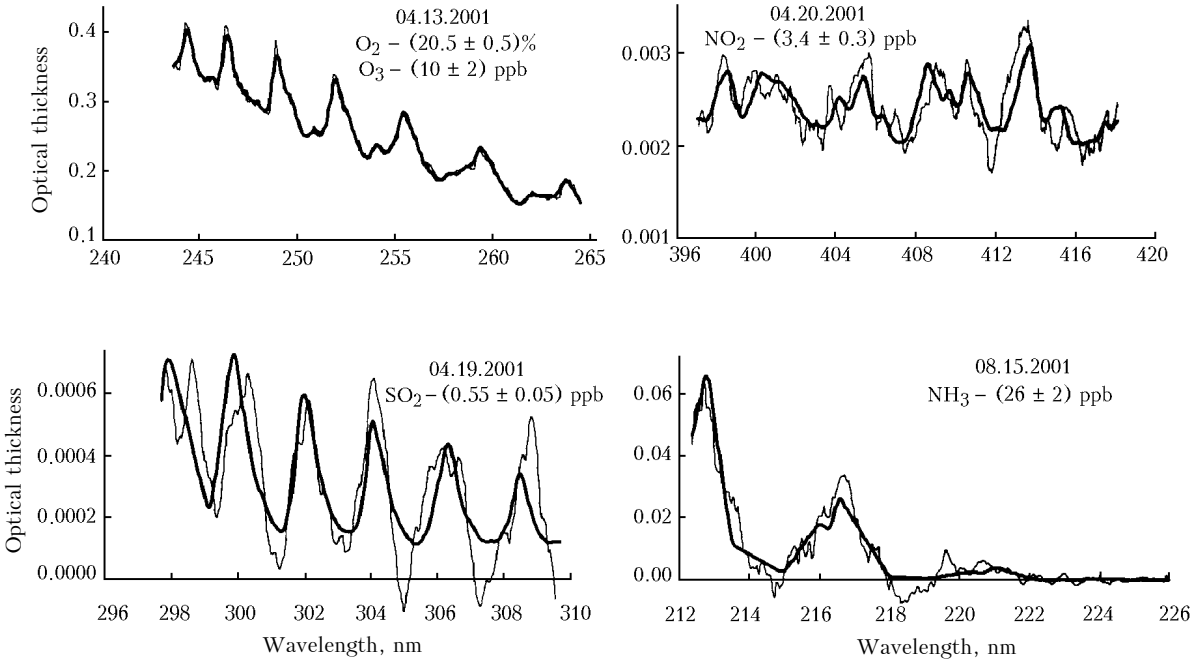

Fig. 3. Experimental absorption spectra for some gases obtained along an open atmospheric path in Obninsk (thin curves) as compared with calculated data (bold curves).

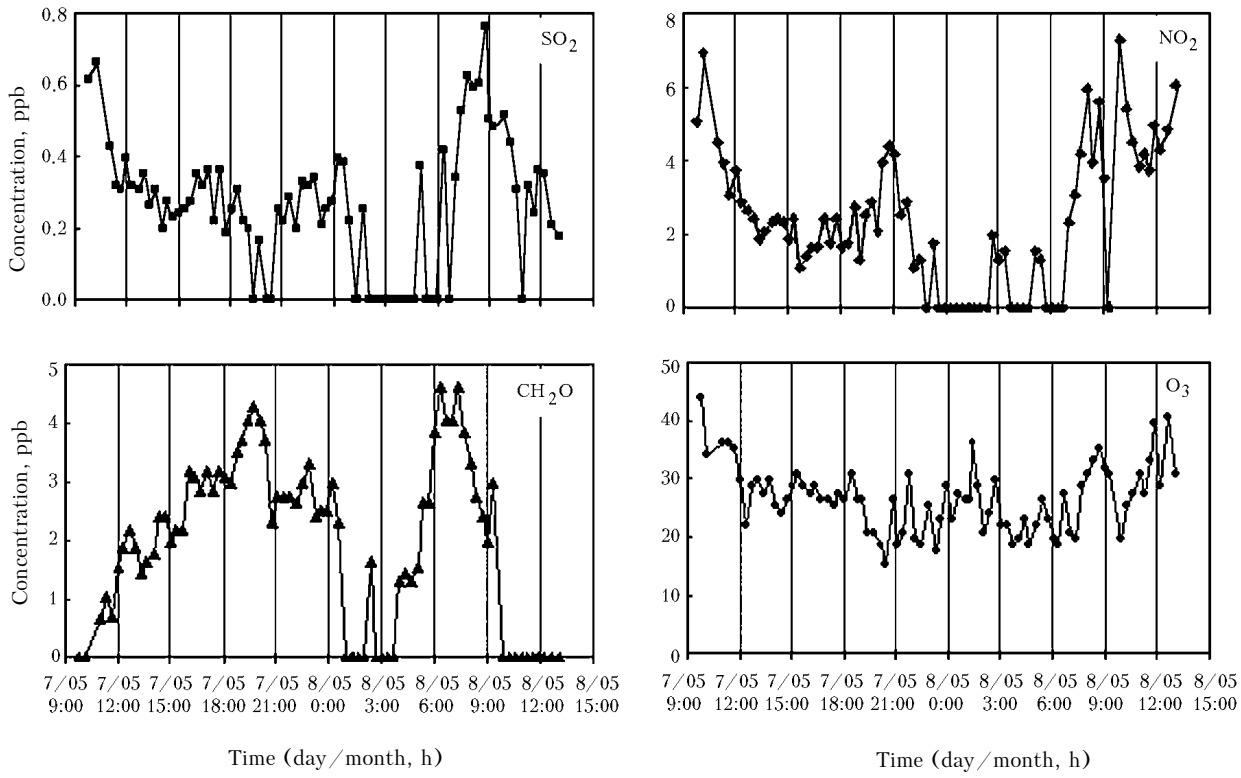

Fig. 4. 24-hour measurements of gas concentrations in Obninsk on May 7–8, 2001.

– O_3. The maximum concentrations at the level of 60–80 ppb were observed in the period of 11:00–13:00 LT on sunny days, when the temperature inversion was observed in the layer of 100–300 m until 12:00 (April 24–26). The minimum concentrations from 5 to 9 ppb were observed during rain – from 13:00 to 15:00 on May 11.

The DOAS-4R is now fully automated. Tests including continuous measurements for several days were conducted in Moscow. The results of these tests will be published in our next paper.

Conclusion

The first domestic produced open path gas analyzer DOAS-4R has been designed and tested. The DOAS-4R gas analyzer can be used for monitoring of gas pollutants in the urban atmosphere. DOAS-4R is capable of acquiring measurement data in real time, and thus it can be employed in automated hazardous pollution warning systems. Since several gaseous components are measured simultaneously, DOAS-4R can yield valuable information in investigations connected with the transport and transformation of gas pollutants in the atmosphere. The DOAS-4R detection limit is from tenths of ppb to a few ppb at the measurement time of 2–3 min.

Acknowledgments

The authors are indebted to V.S. Khmelevtsov, who contributed significantly to software development, and D.I. Busygina for her help in preparation of this paper.

References

1. U. Platt, in: *Air Monitoring by Spectroscopic Techniques*, ed. by M.W. Sigrist, Chem. Analys. Series. Vol. 127 (1994), pp. 27–84.

2. J. Stutz and U. Platt, Appl. Opt. **36**, No. 6, 6041–6053 (1997).

3. G. Strang, *Linear Algebra and Its Applications* (Harcourt Brace Jovanovich, San Diego, 1988).

4. P. Bernath, M. Carleer, S. Fally, et al., Chem. Phys. Lett. **297**, 293–299 (1998).

5. A. Jenouvrier, M.-F. Merienne, B. Coquart, et. al., J. Mol. Spectrosc. **198**, 136–162 (1999).

6. M.-F. Merienne, A. Jenouvrier, B. Coquart, et al., J. Mol. Spectrosc. **202**, 171–193 (2000).

7. Th. Etzkorn, B. Klotz, S. Sórensen, et al., Atmos. Environ. **33**, 525–540 (1999).

8. F.Ya. Rovinskii and V.I. Egorov, *Ozone, Nitrogen, and Sulfur Oxides in the Lower Atmosphere* (Gidrometeoizdat, Leningrad, 1986), 183 pp.